Electrical Power and Energy Systems 43 (2012) 1443–1452

Contents lists available at SciVerse ScienceDirect

Electrical Power and Energy Systems

journal homepage: www.elsevier.com/locate/ijepes

# A computational study of a stochastic optimization model for long term hydrothermal scheduling

Vitor Luiz de Matos *, Erlon Cristian Finardi

*LabPlan – Laboratório de Planejamento de Sistemas de Energia Elétrica, Campus Universitario, Trindade, Florianópolis, SC, CEP 88040-900, Brazil*

ARTICLE INFO

*Article history:*
Received 22 April 2010
Received in revised form 18 May 2012
Accepted 2 June 2012
Available online 9 August 2012

*Keywords:*
Long-term hydrothermal scheduling
Multi-stage stochastic linear programming
Energy Equivalent Reservoir
Periodic Autoregressive model
Stochastic Dual Dynamic Programming

ABSTRACT

The long-term hydrothermal scheduling is one of the most important problems that must be solved in power systems area. This problem aims to obtain an optimal policy, under water resources uncertainty, for the hydro and thermal plants over a multi-annual planning horizon. The purpose of this paper is two-fold. Firstly, we present a computational model which is in development for solving the long-term hydrothermal scheduling of the Brazilian hydrothermal power system. Secondly, it is described some modeling issues which may cause problems to achieve an optimal policy and are currently included in the official long-term optimization model of the Brazilian regulatory framework. This paper presents some solutions, for those problems, that were implemented on our model. We evaluate the solutions related to the original modeling and the modified one, in order to show evidences of the problems and that the solutions proposed are a good start point. To accomplish this evaluation, we consider in the model the whole Brazilian power system, with a reduced planning horizon.



## 1. Introduction

In a hydrothermal system with hydro resource predominance, the hydrothermal scheduling problem is a very complex task, given that all the particularities related to this problem cannot be accommodated in a single optimization model. In order to deal with this task, a chain of models is normally used, dividing the main problem into a hierarchy of smaller subproblems with different planning horizons and degrees of detail. Then, some information from the long-term scheduling problem [1,2] is used as input to the more detailed mid-term problem [3–5] which, in turn, feed their results into the short-term scheduling problem [6–11]. The information transferred from one problem to other can be some target of generation [12] or a function that describes the future operation cost with respect the storage level of water in the reservoirs [13].

In the long-term hydrothermal scheduling problem (LTHS), which is the focus of discussion in this paper, the main objective is to obtain a optimal policy that minimize the operation cost over a planning horizon, that considers 5–10 years, taking into account constraints related to the system and power plants. In this horizon, the model needs to take into consideration the water inflow seasonality and uncertainty, and the possibility to transfer water over the time by managing the reservoirs. Thus, depending on the electrical industry regulatory framework, the solution of this problem is useful for the Independent System Operator (ISO) or by the generation companies that own a mix of hydro and thermal plants, and need to submit bids (price and quantity) to the ISO.

Particularly, in the Brazilian hydrothermal power system, the ISO is responsible for the hydrothermal scheduling of the system and, as a consequence, it uses a chain of optimization models. In this context, LTHS problem is solved by a model called NEWAVE [14]. The main result of this model is the future cost function (FCF) which represents the system operation costs in the future as a function of the stored water and the water inflow.[1] This FCF is used as boundary condition in the subsequent optimization model in the chain.

Several models have been proposed for solving the LTHS problem [15–22]. However, most of them [15–20] do not consider the specific characteristics of the Brazilian hydrothermal power system. Furthermore, NEWAVE has been continuously improved in order to comply with the growing requirements of the industry. Thus, based on our experience in other stochastic models [3,23–26], we are developing a model, called SMERA (Stochastic Model for Energy Resource Allocation), which allow us to suggest some improvements with respect the current model used in Brazil.

As it is detailed ahead, the LTHS is a large scale linear stochastic optimization problem, with temporal and spatial coupling. The stochastic characteristic arises from the fact that it is impossible to

* Corresponding author. Tel.: +55 48 37219731; fax: +55 48 37217538.
*E-mail addresses:* vitor@plan4.com.br (Vitor Luiz de Matos), erlon.finardi@ufsc.br (E.C. Finardi).

[1] In reality, the NEWAVE model convert stored water in the reservoir and the water inflow into stored energy and energy inflow, respectively, as it can be seen in the Section 3.1.

0142-0615/$ - see front matter © 2012 Elsevier Ltd. All rights reserved.
http://dx.doi.org/10.1016/j.ijepes.2012.06.021

forecast future inflows accurately, and so these inflows are modeled as random variables with a known probability distribution. The temporal coupling is explained by the fact that the water can be managed over the time, observing the storage capacity of each reservoir. The spatial coupling is due to the fact that the dispatch of a particular hydro plant alters the inflow to the downstream plants, for example. The problem is represented by a linear model, because in this planning horizon (5–10 years) it is more important to represent the inflows uncertainties than the nonlinearities associated with hydro production and thermal costs [6]. Finally, the LTHS problem is considered to be a large scale problem due to the large number of hydro plants and time stages.

To include all the characteristics aforementioned, SMERA has being developed based on three main structures: (i) the Energy Equivalent Reservoir (EER) that aggregates a set of hydro plants in a smaller number of equivalent reservoirs in order to reduce the size of the optimization problem. In this case, the decisions variables are presented in terms of energy instead of water; (ii) the Periodic Autoregressive (PAR) model to generate the inflows scenarios; and (iii) the Stochastic Dual Dynamic Programming (SDDP) algorithm, responsible for calculating the optimal policy. These structures are detailed in the Section 3.

The first main contribution of this paper is offered by means of a discussion of the modeling used in the Brazilian LTHS problem. The EER and PAR models in use add nonlinearities to the problem, and as it can be seen in the computational results, these nonlinearities make the optimization problem nonconvex. The main consequence is that the SDDP cannot find an optimal policy, since this algorithm needs to solve a convex problem to find the optimal solution. The second main contribution is to present one strategy to deal with the EER's nonlinearities and two alternative approaches for the PAR model.

The paper is organized as follows. In Section 2 we present a brief stochastic programming discussion just to introduce the reader some important concepts with respect to the scenarios tree. Then, Section 3 presents the modeling for the LTHS, more precisely, it is discussed the EER, the PAR model, and the SDDP algorithm. Section 4 highlights the nonlinear characteristics and how we are dealing with them in SMERA. Section 5 presents the results and analysis of the cases in study. Section 6 presents the final remarks.

## 2. Stochastic programming

In stochastic programming, uncertainty is modeled by random variables with known probability distributions. In a precise way, the random variables should be modeled by a continuous distribution, making it usually impossible to solve the problem [27]. In order to overcome this difficulty, the distribution is either discretized or sampled, for instance, by means of a Monte Carlo technique. Even in this case, the resulting problem may be very difficult to solve, given that it is necessary to find the optimal solution considering all realizations that were discretized or sampled from the probability distribution function.

Firstly, we present the two-stage stochastic programming problem, in which a decision needs to be made at the first stage without knowing the realization of the random variable in the second stage. In order to make this decision, all possible realizations in the second stage need to be considered by the first stage. This structure can be easily shown as a simple scenario tree, Fig. 1, in which each node at the second stage represents a possible realization.

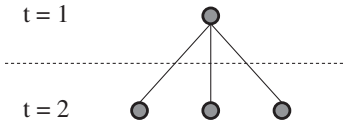


**Fig. 1.** Two-stage scenario tree.

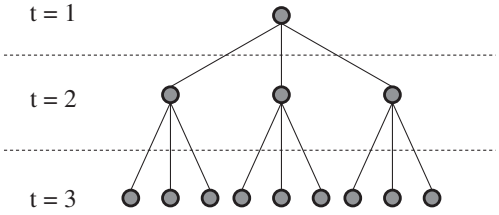


**Fig. 2.** Multi-stage scenario tree.

Secondly, in a multi-stage setting, we must make decisions at each stage and evaluate the consequences in the following one. An example of a scenario tree in multi-stage setting is illustrated by Fig. 2. In this figure each node has a decision to be made, in which all descendent nodes (realizations) need to be taken into account. This feature explains the reason why the scenario tree grows exponentially with the number of stages; for instance, a scenario tree with $T$ stages and $n$ realizations has $n^{T-1}$ nodes in the last stage. In this figure, a scenario is a full path from stage 1 to stage $T$; thus the number of scenarios is exactly the same as the number of nodes in the last stage.

## 3. SMERA model

The first important structure in the model is the representation of the reservoirs, in which a particular set of hydro plants are modeled as a single one by using the concept of Energy Equivalent Reservoir (EER). The second one is the Periodic Autoregressive (PAR) model, which is responsible for generating the scenario tree. The last one is strategy to solve the LTHS problem that is the Stochastic Dynamic Dual Programming (SDDP). All these structures are discussed in the following. The purpose is only to offer to the reader a minimum base to the better comprehension of the SMERA as whole.

### 3.1. Energy Equivalent Reservoir

According to Arvanitidis and Rosing [28], the EER is most applicable when the sequence of monthly decisions on the total hydro production is more important than the allocation of this total among the hydro plants. This modeling is necessary in the Brazilian case in order to reduce the computational burden, due to the large number of hydro power plants.[2]

The main attributes of the EER are illustrated in Fig. 3. Table 1 presents all EER attributes, with their notation and a very brief description. The equations used in the model are presented in [25,29]. Basically, the EER attributes are calculated by the energy that could be produced by using the water associated with each one of the attributes presented in Table 1. In order to find the equivalent energy, the volume of water is multiplied by the sum of the average productivity of all hydro plants in the cascade through which the water flows.

The energy generated in a hydro plant is related to the transformation of the gravitational energy in kinetic energy in the turbines and, consequently, the hydro plant generation depends on its water net head. Therefore, some of the EER attributes are

[2] In the SMERA, the hydro plants can be aggregated per electrical subsystem or per cascade [25]. An electrical subsystem is a region in which the transmissions limits may be ignored in long term studies. In Brazil there are four electrical subsystems: Southern, Southeastern, Northeastern and Northern.

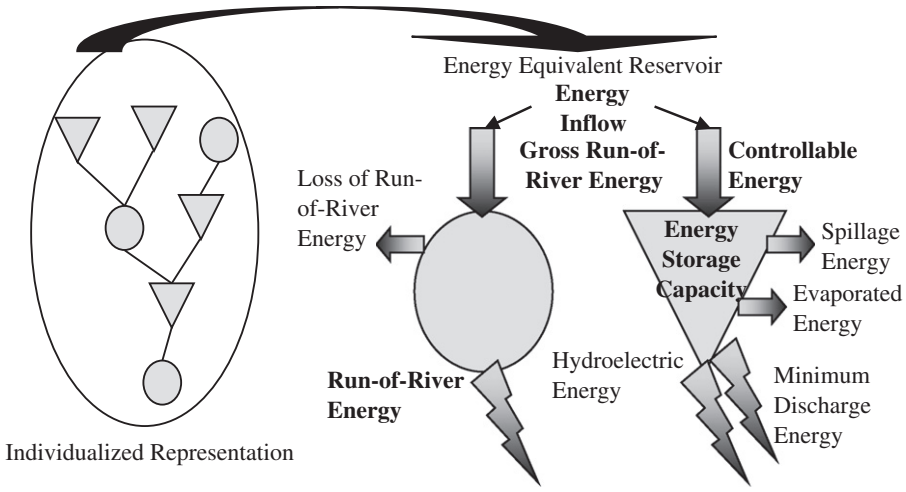


**Fig. 3.** Energy Equivalent Reservoir main attributes.

**Table 1**
EER attributes*.

| Name | Notation | Description (energy that can be generated by…) |
|---|---|---|
| Stored energy | $v$ | The volume stored in the reservoirs |
| Maximum stored energy | $v^{\max}$ | The maximum volume of the reservoirs |
| Minimum stored energy | $v^{\min}$ | The minimum volume of the reservoirs |
| Controllable Energy Inflow | $yc$ | The reservoirs' inflows, this energy can be stored in the EER |
| Gross run-of-river energy inflow | $yb$ | The run-of-river hydro plants inflows without considering the operation limits, which cannot be stored. |
| Loss of run-of-river energy inflow | $yp$ | The losses in run-of-river hydro plants due to operation limits. |
| Run-of-river energy inflow | $yf$ | The run-of-river hydro plants inflows considering the operation limits, i.e., $yf = yb - yp$ |
| Energy inflow | $y$ | All hydro plants inflows, i.e., $y = yc + yb$ |
| Evapored energy | $ev$ | The water evaporated from the reservoirs |
| Minimum discharge energy | $q^{\min}$ | The reservoirs' minimum water discharge |
| Production before the full commitment | $ec$ | The hydro plants that have just been constructed, but it does not have all units committed |
| Fulfilling minimum stored energy | $vm$ | The water necessary to fulfill the new hydro plants' reservoir up to its minimum volume |
| Energy controllable inflow deviation | $qc$ | The water deviated just before the reservoirs |
| Energy run-of-river inflow deviation | $qf$ | The water deviated just before the run-of-river plants |
| Maximum energy generation | $gh^{\max}$ | The reservoirs' maximum water discharge. |
| Spillage energy | $s$ | The water spilled |

* The unit of all attributes is MWmonth, which is the equivalent to a constant generation or consumption through the whole month.

calculated considering the water net head variation, which is a function of the stored volume (stored energy). As a result, these attributes are defined as a function of the stored energy ($v$) and are calculated by fitting a function in three values of the respective attribute and $v$. The functions are assumed to be quadratic and they are presented below.

$$q_{rt}^{\min} = bq_{r2}\, v_{rt}^2 + bq_{r1}\, v_{rt} + bq_{r0}, \tag{1}$$

$$eV_{rt} = be\, v_{r2}\, v_{rt}^2 + be\, v_{r1}\, v_{rt} + be\, v_{r0}, \tag{2}$$

$$gh_{rt}^{\max} = bgh_{r2}\, v_{rt}^2 + bgh_{r1}\, v_{rt} + bgh_{r0}, \tag{3}$$

$$f_{crt} = bf_{r2}\, v_{rt}^2 + bf_{r1}\, v_{rt} + bf_{r0}, \tag{4}$$

where $v_{rt}$ is the stored energy in the EER $r$ and stage $t$; $q_{rt}^{\min}$ the Minimum Discharge Energy of the EER $r$ and stage $t$; $bq_{rk}$ the $q^{\min}$ constant of the order $k$, with $k = 0$, 1 and 2; $ev_{rt}$ the Evaporated Energy of the EER $r$ and stage $t$; $bev_{rk}$ the $ev$ constant of the order $k$, with $k = 0$, 1 and 2; $gh_{rt}^{\max}$ the maximum hydraulic generation of the EER $r$ and stage $t$; $bgh_{rk}$ the $gh^{\max}$ constant of the order $k$, with $k = 0$, 1 and 2; $fc_{rt}$ the Correction Factor of the Controllable Energy of EER $r$ in stage $t$; and $bf_{rk}$ *is the* $fc$ constant of the order $k$, with $k = 0$, 1 and 2.

In the same way that the four attributes aforementioned depends on the stored energy, the Controllable Energy Inflow also depends on the hydro plant's net head. However, the $yc$ is obtained as a by-product of the Energy Inflow and the correction cannot be made as in (1)–(4). As a consequence, it is added another attribute to the EER that adjusts $yc$ according to the stored energy, which is called Correction Factor for the Controllable Energy Inflow ($fc$).

### 3.2. Periodic Autoregressive model

The PAR model, which uses information from $p$ previous months, is responsible for generating the Energy Inflows, which describe the scenario tree to be solved by the LTHS problem. According to Noakes et al. [30], this model is the most suitable tool to forecast monthly inflows. The PAR model was developed to model periodic time series, in which the PAR model's residual are independent and follow a normal distribution [31]. Particularly, in the case of the historical Energy Inflows, the assumption of normality for the residuals does not work well and the model fails to reproduce the log-normal distribution, which is the most useful for these data [25,29,30]. For this reason, a possible approach should

be to make a Box–Cox transformation,[3] which was used by Noakes et al. [30], on the historical data [22] and then an inverse transformation is applied to the forecasted inflows in order to have the correct inflows. However, these transformations are nonlinear and, then, cannot be used in our case, as discussed in Section 3.4.

To overcome this difficulty, in this paper, as suggested by [29], the PAR model was applied directly to the original historical data, without the Box–Cox transformation. Nevertheless, as the model does not reproduce the distribution of the historical Energy Inflow, some adjustments are needed to be made on the residuals. In order to explain this adjustments more appropriately, let us assume the following PAR model, in which the residual has a normal distribution.

$$\left(\frac{y_{m+S\cdot(t-1)}-\mu^{(m)}}{\sigma^{(m)}}\right)=\phi_1^{(m)}\left(\frac{y_{m+S\cdot(t-1)-1}-\mu^{(m-1)}}{\sigma^{(m-1)}}\right)+\cdots+\phi_{Pm}^{(m)}\left(\frac{y_{m+S\cdot(t-1)-Pm}-\mu^{(m-Pm)}}{\sigma^{(m-Pm)}}\right)+\kappa^N_{m+S\cdot(t-1)}, \tag{5}$$

where $y_t$ is the non-normal periodic time series; $S$ the number of seasons. In this case $S=12$; $\mu^{(m)}$ the average of $y_t$ in the month $m$; $\sigma^{(m)}$ the standard deviation of $y_t$ in the month $m$; $\phi_{Pm}^{(m)}$ the autoregressive coefficient lag-$p_m$ in the month $m$; and $\kappa^N_{m+S\cdot(t-1)}$ is the residual – uncorrelated time series, $N(0,\sigma_a^{(m)^2})$.

The approach proposed in [29] and implemented in the SMERA, consists in replacing the residual with a normal distribution ($\kappa^N_{m+S\cdot(t-1)}$) for a lognormal residual ($\kappa_t$), which is defined in (6). The $\kappa_t$ is a three-parameter log-normal distribution, in which the variable $\xi_t$ in (6) has a normal distribution with zero mean and standard deviation equal to 1. The new uncorrelated time series can be obtained as follows.

$$\kappa_t=\exp(\xi_t\cdot\sigma_\xi^{(m)}+\tau)+\delta. \tag{6}$$

In addition to reproducing the historical data, it is absolutely necessary to guarantee that the PAR model does not generate negative Energy Inflows.[4] As detailed ahead, a strategy which guarantees that the Energy Inflow is always positive consists in the definition of a suitable parameter $\delta$ as:

$$\delta=-\left(\frac{\mu^{(m)}}{\sigma^{(m)}}\right)-\phi_1^{(m)}\left(\frac{y_{m+12\cdot(t-1)-1}-\mu^{(m-1)}}{\sigma^{(m-1)}}\right)-\cdots-\phi_{Pm}^{(m)}\left(\frac{y_{m+12\cdot(t-1)-Pm}-\mu^{(m-Pm)}}{\sigma^{(m-Pm)}}\right), \tag{7}$$

According to [29], the parameters $\tau$ and $\sigma_\xi^{(m)}$ are estimated in a way to maintain the first and second statistical moments of the historical data by means of the following relations:

$$\gamma=1+(\sigma_\kappa^{(m)^2}/\delta^2), \tag{8}$$

$$\sigma_\xi=\sqrt{\ln(\gamma)}, \tag{9}$$

$$\tau=\ln(\sigma_\kappa^{(m)}/\sqrt{\gamma(\gamma-1)}). \tag{10}$$

As a consequence, considering (5) and (6), the PAR model applied to the LTHS problem is:

$$\left(\frac{y_{m+S\cdot(t-1)}-\mu^{(m)}}{\sigma^{(m)}}\right)=\phi_1^{(m)}\left(\frac{y_{m+S\cdot(t-1)-1}-\mu^{(m-1)}}{\sigma^{(m-1)}}\right)+\cdots+\phi_{Pm}^{(m)}\left(\frac{y_{m+S\cdot(t-1)-Pm}-\mu^{(m-Pm)}}{\sigma^{(m-Pm)}}\right)+\exp(\xi_t\cdot\sigma_\xi^{(m)}+\tau)+\delta. \tag{11}$$

### 3.3. The LTHS formulation

The SDDP is a decomposition technique that solves each node, of the scenarios tree, separately; each one is modeled as a LP problem. In this sense, we present the formulation of the LTHS problem for one particular node. The formulation of LTHS problem in the Brazilian case must take into account the EER representation, the PAR model and the load levels.[5]

$$\omega_t=\min\sum_{j=1}^{NUT}\left(ct_j\cdot\sum_{q=1}^{NP}gt_{jqt}\right)+\sum_{k=1}^{NS}\left[\sum_{h=1}^{NDEF}\left(cd_{hk}\cdot\sum_{q=1}^{NP}d_{hkqt}\right)\right]+\frac{1}{(1+\beta/100)}\alpha_{t+1}, \tag{12}$$

s.t.:

$$v_{r,t+1}+\sum_{q=1}^{NP}gh_{rqt}+s_{rt}=f_{rt}v_{rt}-q^{\min}_{rt}+qc_{rt}-vm_{rt}-ev_{rt}+fc_{rt}a_r(\varphi_{rt1}y_{r,t-1}+\cdots+\varphi_{rtp_m}y_{r,t-p_m}+\eta_{rt}+\kappa_{rt}), \tag{13}$$

$$\sum_{r\in NR_k}gh_{rqt}+\sum_{j\in NUT_k}gt_{jqt}+\sum_{n\in\Omega_k}(f_{nkqt}-f_{knqt})+\sum_{h=1}^{NDEF}d_{khqt}+exc_{qkt}=L_{kt}LF_{kqt}FP_{kqt}-\sum_{r\in NR_k}(q^{\min}_{rt}+pu_{rt})FP_{kqt}-\sum_{r\in NR_k}[(1-a_r)(\varphi_{rt1}y_{r,t-1}+\cdots+\varphi_{rtp_m}y_{r,t-p_m}+\eta_{rt}+\kappa_{rt})-yp_{rt}+qf_{rt}]FP_{kqt}, \tag{14}$$

$$gt^{\min}_{jt}FP_{k_jqt}\leqslant gt_{jqt}\leqslant gt^{\max}_{jt}FP_{k_jqt}, \tag{15}$$

$$0\leqslant d_{khqt}\leqslant d^{\max}_{kht}FP_{kqt}, \tag{16}$$

$$0\leqslant f_{nkqt}\leqslant f^{\max}_{nkt}FP_{kqt}, \tag{17}$$

$$0\leqslant f_{knqt}\leqslant f^{\max}_{knt}FP_{kqt}, \tag{18}$$

$$v^{\min}_{rt}\leqslant f_{r,t+1}v_{r,t+1}\leqslant v^{\max}_{rt}, \tag{19}$$

$$0\leqslant gh_{rqt}\leqslant gh^{\max}_{rt}FP_{k_rqt}-[(1-a_r)(\varphi_{rt1}y_{r,t-1}+\cdots+\varphi_{rtp_m}y_{r,t-p_m}+\eta_{rt}+\kappa_{rt})-yf]FP_{k_rqt}-qf_{rt}FP_{k_rqt}-q^{\min}_{rt}FP_{k_rqt}, \tag{20}$$

$$\alpha_{t+1}-\sum_{r\in NR}\pi_{v,r}(v_r-v_r^0)-\sum_{r\in NR}\sum_{p=0}^{Pm-1}\pi_{y,r,p+1}(y_{r,t-p}-y^{sc}_{r,t-p}).\geqslant\alpha^0_{t+1} \tag{21}$$

where *NUT*, *NP*, *NS*, *NDEF*, *NR* are the number of thermal plants, load levels, electrical subsystems, energy deficit levels and EERs; *j, q, k, n, h, r, I* the thermal plants, load levels, electrical subsystems, energy

[3] The Box–Cox transformation is given by: $y_t(\lambda)=\lambda^{-1}[(y_t+c)^\lambda-1]$ when $\lambda\neq0$ and $y_t^{(\lambda)}=\ln(y_t+c)$ when $\lambda=0$, in which $y_t^{(\lambda)}$ is the transformed time series and $c$ is a constant [31].

[4] From (5) one can notice that, the PAR model considers the deviation of the $p$ previous inflows from its average value, if the previous inflows are smaller than its average value and depending on the value of the new uncorrelated time series (6), it is possible to have the negative energy inflows.

[5] The load curve is modeled into three levels: Light (low consumption period), Medium (average consumption period) and Peak (peak load period).

deficit levels, EERs and iterations' indexes; $ct_j$ the thermal plants' $j$ incremental costs (R$/MWmonth); $gt_{jqt}$ the thermal plants' $j$ generations in load level $q$ and stage $t$ (MWmonth); $cd_{hk}$ the energy deficit levels' $h$ incremental costs in subsystem $k$ (R$/MWmonth); $d_{hkqt}$ the energy deficit levels' $h$ generation in subsystem $k$, load level $q$ and stage $t$ (MWmonth); $gh_{rqt}$ the EERs' $r$ generation in load level $q$ and stage $t$ (MWmonth); $a_r$ the coefficient to calculate the controllable part of the energy inflow $y$; $f_{nkqt}$ the energy interchange from electrical subsystems $n$ to $k$ in load level $q$ and stage $t$ (MWmonth); $LF_{kqt}$ the consumption factor[6] of subsystem $k$ in load level $q$ and stage $t$ (%); $FP_{kqt}$ the load level factor of subsystem $k$ in load level $q$ and stage $t$ (%); $exc_{kqt}$ the excess of energy of subsystem $k$ in load level $q$ and stage $t$; $gt_{jt}^{\min}$ the minimum generation of thermal plant $j$ in stage $t$ (MWmonth); $gt_{jt}^{max}$ the maximum generation of thermal plant $j$ in stage $t$ (MWmonth); $d_{kht}^{max}$ the maximum energy assumed by deficit level $h$ of subsystem $k$ in stage $t$ (MWmonth); $f_{nkt}^{max}$ the maximum interchange from electrical subsystems $n$ to $k$ in stage $t$ (MWmonth); $\alpha_{t+1}$ Expected future cost of stage $t+1$ (R$); $\pi_{v,r}$ the cut coefficient associated with the stored energy of EER $r$ (R$/MWmonth); $\pi_{y,r,p+1}$ the cut coefficient associated with the Energy Inflow of EER $r$ and order $p+1$ (R$/MWmonth); and $\beta$ is the discount rate (%).

Eq. (12) represents the objective function, which is subject to the energy reservoir balance constraint for each EER (13), the load supply constraint for each electrical subsystem and load levels (14). The variables' limits are imposed by (15)–(20) and the future cost function is described by (21).

As it can be noticed in the LTHS formulation, we use a compact formula to represent the PAR model when compared with (11), where the constants shown in (13)–(20) are now recalculated as follows:

$$\varphi_{rtp} = \phi_p^{(m)} \sigma^{(m)} / \sigma^{(m-p)} \tag{22}$$

$$\eta_{rt} = \mu^{(m)}/\sigma^{(m)} - \phi_1^{(m)} \mu^{(m-1)}/\sigma^{(m-1)} - \ldots - \phi_{Pm}^{(m)} \mu^{(m-Pm)}/\sigma^{(m-Pm)} \tag{23}$$

### 3.4. Stochastic Dual Dynamic Programming

As aforementioned, in this paper we are not interested in discussing the SDDP algorithm and its performance. In this sense, most of its theoretical discussions, presented thoroughly in [13,29,32], are omitted. However, it is important to explain how the SDDP algorithm constructs its optimal policy.

The SDDP is a sampling-based algorithm for solving stochastic linear problems. The algorithm can be divided into two steps: forward and backward passes. In the forward pass, the algorithm samples a group of scenarios (full path from the first to the last stage) from the scenario tree; then, it optimizes each node of these scenarios starting at the first stage and proceeding to the next one until it solves the last stage. In the backward pass, the algorithm starts at the last stage and add information to the previous stage with respect to the operation future cost (a Benders Cut) until the first stage is reached. The Benders cut (21) is a linear approximation of the future cost and measures how much the future cost depends on the amount of water that will be available in the beginning of the next time stage. In order to finish this process, a suitable convergence criterion is used.

[6] The consumption factor is a value for each load level and electrical subsystem that multiplies the demand in order to have the energy to be supplied in the light, average and heavy periods of consumption. The sum of the three load level factors multiplied by its consumption factors must be equal to 100%, in each electrical subsystem.

In order to guarantee an unbiased estimator of the operation costs, it is necessary to sample new scenarios from the scenario tree at each iteration. If the convergence was not reached yet, it is add new information about the future in the backward pass, which is followed by a new forward pass. The algorithm continues to perform the forward and backward passes until the convergence is reached. The convergence is achieved when the expected operation cost at the first stage, which is the sum of the present and future cost, is statistically equal to the expected total operation cost, which corresponds to the sum of all expected operation cost for each time stage, considering the economic discount rate. The first value is known as the Lower Bound and the latter is the Upper Bound. More details on these values can be found in [13,29,32].

One important characteristic of the SDDP that needs to be discussed in this paper is the cut sharing. In the SDDP, the Benders cut must be shared among all nodes in the stages; this means that a cut created for a particular scenario, at stage $t$, must be added to all nodes in the stage $t$. Therefore, instead of adding one cut in each scenario per iteration, the SDDP adds $N$ cuts per iteration, where $N$ is the number of sampled scenarios in the forward pass. The cut sharing is necessary due to the following reasons:

(i) To guarantee that a particular node in different scenarios, in the forward passes, presents the same decision. This property can be ensured only if the node, in the different scenarios, has the same future cost function.
(ii) Due to the re-sampling process at each iteration, when a scenario is sampled for the first time some of its nodes do not have any information on the future cost. Thus, if the cuts were not shared, the SDDP would need many more iterations to achieve the convergence, therefore, the SDDP would be computationally infeasible.
(iii) If the cuts were not shared, each node would have a particular future cost function. However, it is necessary to have only one future cost function in each stage, given that the future cost function is used to couple the long and medium-term operation planning models in the Brazilian case.

In order to share the cuts among the scenarios [33], the main requirement is presented in Fig. 4, in which the scenario tree must have common samples [34]. In a scenario tree with common samples, a single set of observations is sampled for each stage and the set is the same for all nodes of the same stage. In Fig. 4, there are four set of observations, one for each stage, $\{\xi_1^a\}, \{\xi_2^a, \xi_2^b, \xi_3^c\}$, $\{\xi_3^a, \xi_3^b\}$ and $\{\xi_4^a, \xi_4^b, \xi_4^c, \xi_4^d\}$.

In the PAR model, the Energy Inflow is a function of one or more previous inflows plus a residual. In this case, the observation $\xi_4^c$ generates different Energy Inflow according to the visited previous

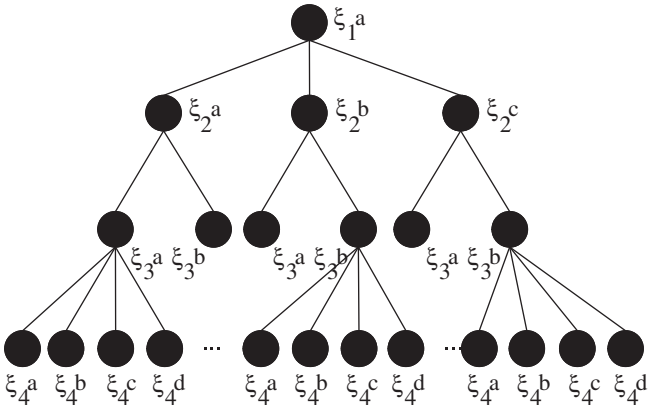


**Fig. 4.** Scenario tree with common samples.

nodes (its scenario). As a consequence, when considering the PAR model and sharing cuts, the random variable $\xi$ refers to the residuals and the previous Energy Inflows must be considered as state variables in the problem.[7]

In order to help the reader to follow the Benders cut calculation, it is presented the objective function of the dual problem for a generic node of the scenario tree. This function is the basis for the computation of the Benders cut coefficients.

$$\begin{aligned} z_t = {} & \lambda_t^T f_t v_t - \lambda_t^T q_t^{\min} - \lambda_t^T eV_t + \lambda_t^T [fc_t a(\varphi_{t1} y_{t-1} + \cdots + \varphi_{tp} y_{t-p} \\ & + \eta_t + \kappa_{rt})] + \lambda_t^T qc_{rt} - \lambda_t^T vm_t + v_t^T L_t LF_t FP_t \\ & - v_t^T \sum_{r \in NR_k} q_{rt}^{\min} FP_{kqt} - v_t^T \sum_{r \in NR_k} pu_{rt} FP_{kqt} - v_t^T \sum_{r \in NR_k} [(1-a) \\ & \times (\varphi_{t1} y_{t-1} + \cdots + \varphi_{tp} y_{t-p} + \eta_t + \kappa_{rt}) - yf_t + qf_{rt}] FP_{kqt} \\ & - \gamma_t^T [(1-a)(\varphi_{t1} y_{t-1} + \cdots + \varphi_{tp} y_{t-p} + \eta_t + \kappa_{rt}) - yf_t] FP_t \\ & + \gamma_t^T gh_t^{\max} FP_t - \gamma_t^T q_t^{\min} FP_t - \gamma_t^T qf_t FP_t + \chi_t^T \alpha^0 \\ & + \chi_t^T \sum_{r \in NR} \pi_{es,r} (v_{rt} - v_r^0) + \chi_t^T \sum_{r \in NR} \sum_{p=0}^{p_{m-1}} \pi_{y,r,p+1} (y_{r,t-p} - y_{r,t-p}^{sc}) \\ & + \psi_t^T v_t^{\max} + \psi_t^T f_t^{\max} FP_t + \psi_t^T f_t^{\max} FP_t - \psi_t^T gt_t^{\min} FP_t \\ & + \psi_t^T gt_t^{\max} FP_t + \psi_t^T d_t^{\max} FP_t, \end{aligned} \tag{24}$$

where $\lambda_t$ is the dual variables vector related to the energy reservoir balance constraints (13); $v_t$ the dual variables vector related to the Load supply constraints (14); $\gamma_t$ the dual variables vector related to the Maximum hydro generation constraints (20); $\chi_t$ the dual variables vector related to the Benders' Cut (21); and $\psi_t$ is the dual variables vector related to the other constraints (15)–(20).

The RHS of the Benders cut ($\alpha_{t+1}^0$) is the expected cost at the iteration that the cut was generated. The coefficients in the second ($\pi_{v,r}$) and third ($\pi_{y,r,p+1}$) term of left hand side measure the cost variation when the state variables vary and their values can be obtained by the differentiation of the dual objective function in relation to the state variables:

$$\begin{aligned} \pi_{v,r} = {} & \frac{\partial z_t}{\partial v_{rt}} = \lambda_{rt} \frac{\partial (f_{rt} v_{rt})}{\partial v_{rt}} + \lambda_{rt} \frac{\partial (fc_{rt})}{\partial v_{rt}} a_r \\ & \times (\varphi_{rt1} y_{r,t-1} + \cdots + \varphi_{rtp_m} y_{r,t-p_m} + \eta_{rt} + \kappa_{rt}) \\ & - \lambda_{rt} \frac{\partial (q_{rt}^{\min})}{\partial v_{rt}} - \lambda_{rt} \frac{\partial (eV_{rt})}{\partial v_{rt}} - \left( \sum_{q=1}^{NP} (v_{k_r qt} FP_{k_r qt}) \right) \left[ \frac{\partial (q_{rt}^{\min})}{\partial v_{rt}} \right] \\ & + \left( \sum_{q=1}^{NP} (\gamma_{rqt} FP_{k_r qt}) \right) \left[ \frac{\partial (gh_{rt}^{\max})}{\partial v_{rt}} - \frac{\partial (q_{rt}^{\min})}{\partial v_{rt}} \right] \\ \pi_{v,r} = {} & \lambda_{rt} f_{rt} + \lambda_{rt} (2bf_{r2} v_{rt} + bf_{r1}) a_r (\varphi_{rt1} y_{r,t-1} + \cdots \\ & + \varphi_{rtp_m} y_{r,t-p_m} + \eta_{rt} + \kappa_{rt}) - \lambda_{rt} (2bq_{r2} v_{rt} + bq_{r1}) \\ & - \lambda_{rt} (2be v_{r2} v_{rt} + be v_{r1}) - \left( \sum_{q=1}^{NP} (v_{k_r qt} FP_{k_r qt}) \right) (2bq_{r2} v_{rt} + bq_{r1}) \\ & + \left( \sum_{q=1}^{NP} (\gamma_{rqt} FP_{k_r qt}) \right) [(2bgh_{r2} v_{rt} + bgh_{r1}) - (2bq_{r2} v_{rt} + bq_{r1})] \end{aligned} \tag{25}$$

Given that some of the EER attributes are described by a quadratic function, one can notice that the cut's coefficient in (25) is a linear function of the stored energy, $v$. However, by analyzing (21) it is possible to see that the cut's coefficient is multiplied by the stored energy, which results a quadratic term (nonlinear) in the Benders cut. In order to avoid this nonlinearity, the NEWAVE model replace the stored energy variable, $v_{rt}$, in (25) by its current value, which correspond to the stored energy in the beginning of the stage at the scenario that the cut was created [29]. This is strategy may create imprecise cuts and the obtained results may be not valid, as presented in Section 5. Possible solutions to deal with this shortcoming are discussed in Section 4.

Following the same idea as in (25), the coefficients calculation, related to the energy inflow, is defined in (26).

$$\begin{aligned} \pi_{y,r,p} = \frac{\partial z_t}{\partial y_{r,t-p}} = {} & \lambda_{rt} a_r fc_{rt} \varphi_{rtp} + \chi_{rt} (\pi_{y,r,1} \varphi_{rtp} + \pi_{y,r,p+1}) \\ & - \left( \sum_{q=1}^{NP} (v_{k_r qt} FP_{k_r qt}) \right) [(1-a_r) \varphi_{rtp}] \\ & - \left( \sum_{q=1}^{NP} (\gamma_{rqt} FP_{k_r qt}) \right) [(1-a_r) \varphi_{rtp}]. \end{aligned} \tag{26}$$

## 4. Nonlinear characteristics

As discussed previously, the SMERA is a linear model and its solution algorithm is based on this characteristic. More precisely, to use the SDDP algorithm the problem must be convex. However, as it is pointed out in this section, there are some nonlinearities that yields a nonconvex problem. These nonlinear characteristic are within the EER and PAR model.

### 4.1. EER

In the EER, the nonlinearities are related to the quadratic functions used to model some of its attributes, such as the Minimum Discharge Energy and the Evaporated Energy. These functions, presented in Section 3.1, add nonlinear characteristics to the problem because the stored energy is our problem's state variable. A very simple solution to solve this issue consists in fitting a linear equation instead of a quadratic, as way to solve a convex problem.

In order to evaluate the proposed linearization, Table 2 presents the $R$-square measure of fitting linear equations. The $R$-square for the quadratic case is 1, once we are fitting a quadratic function based on only three points. The values from the table below show that the linear approximation produces $R$-square close to 1, which indicates that the linear approach could be considered good enough.

### 4.2. PAR model

In the PAR model, the nonlinearity is not as clear as the EER. For this reason, a few rearrangements are made for a better comprehension. We start by substituting (6) in (5) which results in the following expression:

$$\begin{aligned} \left( \frac{y_{m+S\cdot(t-1)} - \mu^{(m)}}{\sigma^{(m)}} \right) = {} & \phi_1^{(m)} \left( \frac{y_{m+S\cdot(t-1)-1} - \mu^{(m-1)}}{\sigma^{(m-1)}} \right) + \cdots \\ & + \phi_{Pm}^{(m)} \left( \frac{y_{m+S\cdot(t-1)-Pm} - \mu^{(m-Pm)}}{\sigma^{(m-Pm)}} \right) \\ & + \exp(\xi_t \cdot \sigma_{\xi}^{(m)} + \tau) + \delta. \end{aligned} \tag{27}$$

Then, by isolating $y_{m+S(t-1)}$ in the left hand side:

$$\begin{aligned} \frac{y_{m+S\cdot(t-1)}}{\sigma^{(m)}} = {} & \frac{\mu^{(m)}}{\sigma^{(m)}} + \phi_1^{(m)} \left( \frac{y_{m+S\cdot(t-1)-1} - \mu^{(m-1)}}{\sigma^{(m-1)}} \right) + \cdots \\ & + \phi_{Pm}^{(m)} \left( \frac{y_{m+S\cdot(t-1)-Pm} - \mu^{(m-Pm)}}{\sigma^{(m-Pm)}} \right) + \exp(\xi_t \cdot \sigma_{\xi}^{(m)} + \tau) + \delta. \end{aligned} \tag{28}$$

[7] If the PAR model was applied to the historical data after the Box-Cox transformation, it would be necessary to perform a nonlinear inverse transformation in the previous Energy Inflows, which would add nonlinearities to the LTHS problem. For this reason, we used the PAR model presented in Section 3.2.

**Table 2**
*R*-square for the linear approximation.

| Attributes | Electrical subsystem | | | |
|---|---|---|---|---|
| | Southeastern | Southern | Northeastern | Northern |
| $q^{\min}$ | 0.931 | 0.943 | 0.926 | 0.910 |
| $ev$ | 0.998 | 0.989 | 0.998 | 0.999 |
| $gh^{\max}$ | 0.931 | 0.933 | 0.919 | 0.950 |
| $fc$ | 0.933 | 0.942 | 0.926 | 0.910 |

Finally, by substituting (7) in (28) yields:

$$\frac{y_{m+S\cdot(t-1)}}{\sigma^{(m)}} = -\delta + \exp(\xi_t \cdot \sigma_{\xi}^{(m)} + \tau) + \delta \Rightarrow y_{m+S\cdot(t-1)} = \exp(\xi_t \cdot \sigma_{\xi}^{(m)} + \tau)\sigma^{(m)}. \quad (29)$$

From (29) it is clear that the PAR model always generates positive Energy Inflows. Nevertheless, given that the parameters $\tau$ and $\sigma_{\xi}^{(m)}$ are a nonlinear function of the previous Energy Inflows as shown in Section 3.2, this model is nonlinear. In order to overcome this shortcoming, two strategies are presented. In the first one, some adjustments in the PAR model are carried out and, in the second, the PAR model is substituted by a much simpler model, the independent random generation.

#### 4.2.1. PAR with $\delta^{MAX}$

One strategy to overcome the problem presented above is to find a single $\delta$ that guarantee a positive Energy Inflow. One possible approach would be to find out the maximum $\delta$ (defined as $\delta^{\text{MAX}}$), for all scenarios of the problem, which guarantees a positive energy inflows values. Although it is a very simple strategy and easy to implement, it is impossible, in terms of computational burden, to evaluate all scenarios from the scenario tree. For this reason, this value is calculated only for the scenarios sampled from the scenario tree.

Furthermore, calculating a single $\delta^{\text{MAX}}$ for all possible scenarios may yield a value that is too big and it could distort the first and second statistical moments. This can occur because the $\delta$ parameter is added to the uncorrelated time series, as one can see in (6), and, then, the bigger the $\delta$ the bigger the Energy Inflow is. As a result, the PAR model could "forecast" values much bigger than it should; generating problems to the first and second statistical moments, these values would not be close to the historical data ones as desired.

In order to reduce the problems of using a single $\delta^{\text{MAX}}$, we calculate $\delta^{\text{MAX}}$ per stage, which we believe would have more modest values in comparison to the other approach (a single value). However, due to the growth of $\delta^{\text{MAX}}$ with the number of scenarios considered in its calculation, we compute this parameter taking into consideration only the sampled scenarios. As a result, this strategy cannot be considered as a final solution because the stochastic sampling algorithm, SDDP, require re-sampling over the iterations, and the $\delta^{\text{MAX}}$ might not be big enough for all sampled scenarios. Therefore, this is a first suggestion on how to deal with the problem and in this paper we intend to present the problems for additional contribution from researchers to find a more robust solution.

In this sense, to avoid the nonlinearities described previously, the PAR model and the adjustments would have the following equations:

$$\frac{y_{m+S\cdot(t-1)}}{\sigma^{(m)}} = \frac{\mu^{(m)}}{\sigma^{(m)}} + \phi_1^{(m)}\left(\frac{y_{m+S\cdot(t-1)-1} - \mu^{(m-1)}}{\sigma^{(m-1)}}\right) + \cdots + \phi_{Pm}^{(m)}\left(\frac{y_{m+S\cdot(t-1)-Pm} - \mu^{(m-Pm)}}{\sigma^{(m-Pm)}}\right) + \exp(\xi_t \cdot \sigma_{\xi}^{(m)} + \tau) + \delta_t^{\text{MAX}}, \quad (30)$$

#### 4.2.2. Independent model

Another solution for the PAR model issue is to ignore the inter-stage dependency. In this case, the energy inflows are calculated considering a three-parameter lognormal proposed by [35]. Although this solution solves the problem and it is able to reproduce the statistical moments, it does not generate series with the periodic characteristics that are well known in inflows realizations. Therefore, in this paper, the independent model is only considered to assist in the evaluations presented in Section 5.

## 5. Computational tests

In order to evaluate the impact of the nonlinearities in the LTHS problem and the proposed solutions, it is used the whole Brazilian interconnected system (139 hydro and 146 thermal plants). It was considered a 6 months horizon and with two energy inflows per stage, which gives us a scenario tree with 32 scenarios. Obviously, this scenario tree is insufficient to define a good operation policy, but it enables us to enumerate all scenarios[8] and solve it using the SDDP scheme. When we guarantee that all scenarios are part of the *Forward* and *Backward* passes, the upper (Zup) and lower (Zlow) bounds should be exactly the same when the SDDP achieves the convergence, so we have a benchmark.

The energy inflows scenario tree is generated by the following models presented in this paper: (i) independent values; (ii) Modified PAR model[9]; and, (iii) Modified PAR model with $\delta^{\text{MAX}}$. In addition, the EER attributes are modeled by linear and quadratic function. The *yp* correction is not used in none of cases and the *fc* is considered in some them. In Table 3, the cases studied in this paper are shown, which is a combination of all the approaches detailed above.

We present the results for all 10 cases above, considering that each one was run for 10 different seeds, i.e., 10 different scenario trees. This strategy gives us more consistent results, because we are studying cases with a very small scenario tree. In order to solve the LP problems, we used the ILOG CPLEX 11.

In all cases we solved the whole scenario tree and, as a result, the lower and upper bound should meet in the last iteration. For this reason, the difference between the upper and lower bounds is evaluated at the 75th iteration, when the program was stopped in all cases.

To begin our studies, it is important to validate[10] the SMERA model. This is possible by comparing cases 0 and 1, as it can be seen in Fig. 5. In Case 0, we constructed a single LP problem with all scenarios and solved it by using CPLEX 11. This case will be the benchmark because it solves the whole scenario tree problem and finds the optimal solution. The values presented in the Fig. 5 are the difference between the optimal cost of the (Case 0) and the Upper Bound of Case 1. As one can notice the difference is small compared to the total cost which is of the order of $10^7$. Consequently, we can assume that SMERA is working properly. Additionally, in Fig. 6 is illustrated the difference between the upper and lower bound in Case 1, which can be considered to be zero given that the values are of the order $10^7$.

Now we present the results for cases 2 and 3, in which we considered the PAR model proposed in Section 3.2 with EER linear and quadratic approximations, respectively. Although the difference

[8] When enumerating all the scenarios, the SDDP is equivalent to the Nested Decomposition (ND) [36], but it solves more LP problems than ND and it shares the cuts among the scenarios.

[9] The Modified PAR model is the PAR model using the adjustments to guarantee positive Energy Inflows.

[10] The program validation means that the policy generated by the SDDP algorithm yields exactly the same solution as solving the whole scenario tree in a single LP problem.

**Table 3**
Study of Cases.

| Case | Energy Inflow model | EER model | *fc* * | Solution strategy |
|---|---|---|---|---|
| 0 | Independent | Linear | No | Single LP |
| 1 | Independent | Linear | No | SDDP |
| 2 | PAR | Linear | Yes | SDDP |
| 3 | PAR | Quadratic | Yes | SDDP |
| 4 | PAR with $\delta^{MAX}$ | Linear | Yes | SDDP |
| 5 | PAR with $\delta^{MAX}$ | Quadratic | Yes | SDDP |
| 6 | PAR with $\delta^{MAX}$ | Linear | No | SDDP |
| 7 | PAR with $\delta^{MAX}$ | Quadratic | No | SDDP |
| 8 | Independent | Linear | Yes | SDDP |
| 9 | Independent | Quadratic | Yes | SDDP |

* The *fc* correction column indicates in which cases the *fc* were considered.

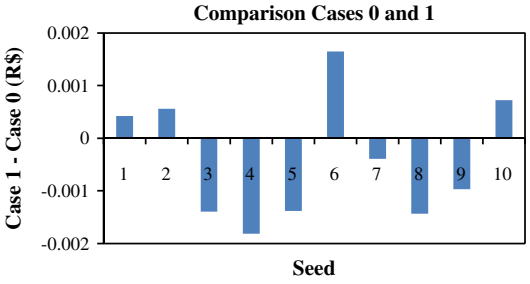


**Fig. 5.** Comparison between Cases 0 and 1.

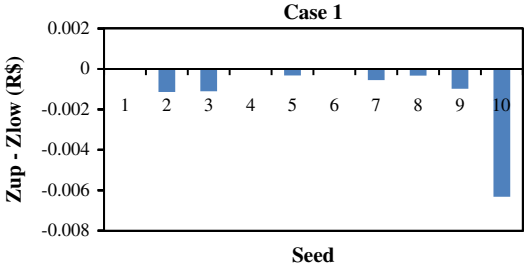


**Fig. 6.** Difference of Zup and Zlow in Case 1.

shown in Fig. 7 is bigger than in Fig. 8, in both cases the difference is much more significant than in the Case 1. This implies that in both cases the SDDP is producing unsatisfactory results; the lower bound becomes greater than the upper.

As it can be noticed in the previous figures, the solution is not adequate and, as we have already validated the SMERA, we need to evaluate different modeling. In this sense, we studied the $\delta^{MAX}$ approach with linear and quadratic approximations of the EER in Figs. 9 and 10, respectively. It is important to point out that the $\delta^{MAX}$ was calculated considering all possible scenarios and, as a consequence, it guarantees positive Energy Inflows and a linear PAR model.

It is possible to notice that the change only in the PAR modeling were not sufficient to guarantee an adequate result even in the case of linear EER attributes. This is because the *fc* correction is still adding nonconvexity to the problem by coupling the stored energy and the energy inflow. For this reason, Figs. 11 and 12 present the results for the $\delta^{MAX}$ strategy without the *fc* correction for the linear and quadratic approximations, respectively.

The results shown in Fig. 11 are satisfactory and indicate that with a proper modeling (linear), the SDDP finds an optimal operation policy. Fig. 12 implies that the nonlinear (quadratic) EER approximations may not be a great issue when the *fc* correction

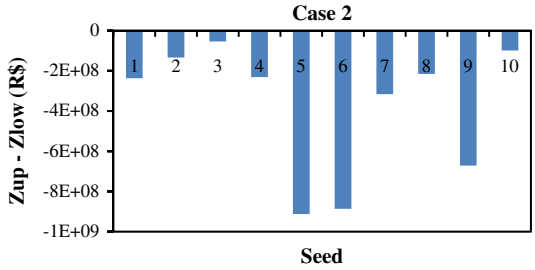


**Fig. 7.** Difference of Zup and Zlow in Case 2.

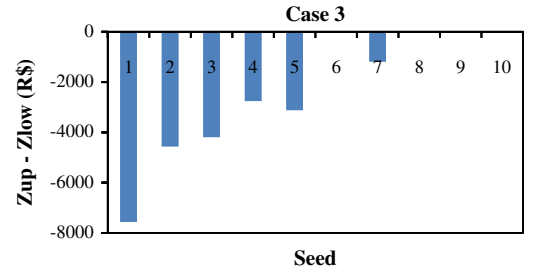


**Fig. 8.** Difference of Zup and Zlow in Case 3.

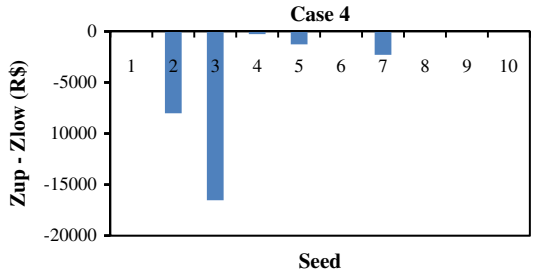


**Fig. 9.** Difference of Zup and Zlow in Case 4.

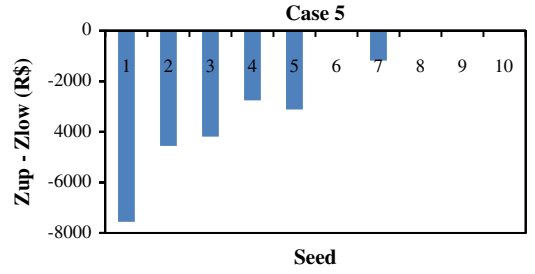


**Fig. 10.** Difference of Zup and Zlow in Case 5.

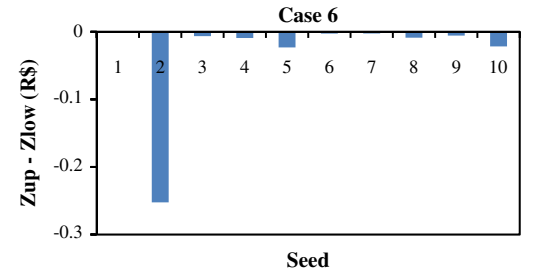


**Fig. 11.** Difference of Zup and Zlow in Case 6.

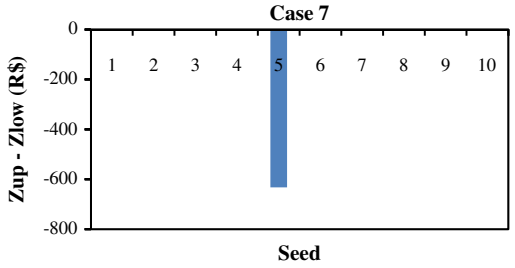


**Fig. 12.** Difference of Zup and Zlow in Case 7.

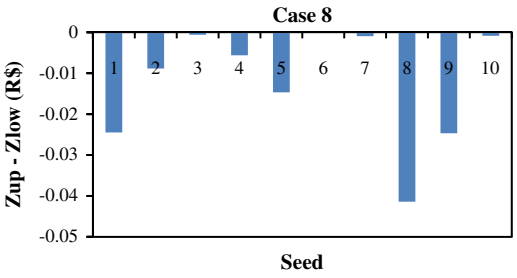


**Fig. 13.** Difference of Zup and Zlow in Case 8.

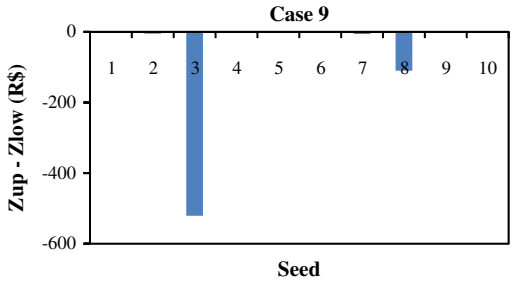


**Fig. 14.** Difference of Zup and Zlow in Case 9.

**Table 4**
Worst result in each case.

| Case | Zup (R$) | Zlow (R$) | Difference (R$) |
|---|---|---|---|
| 1 | $1.54031 \times 10^{6}$ | $1.54031 \times 10^{6}$ | $-6.32000 \times 10^{-3}$ |
| 2 | $7.65413 \times 10^{8}$ | $1.60129 \times 10^{9}$ | $-9.12697 \times 10^{8}$ |
| 3 | $3.04957 \times 10^{7}$ | $3.04999 \times 10^{7}$ | $-4.18866 \times 10^{3}$ |
| 4 | $2.84265 \times 10^{7}$ | $2.84430 \times 10^{7}$ | $-1.65297 \times 10^{4}$ |
| 5 | $1.61764 \times 10^{7}$ | $1.61840 \times 10^{7}$ | $-7.55845 \times 10^{3}$ |
| 6 | $1.44989 \times 10^{7}$ | $1.44989 \times 10^{7}$ | $-2.52484 \times 10^{-1}$ |
| 7 | $1.27061 \times 10^{8}$ | $1.27062 \times 10^{8}$ | $-6.32324 \times 10^{2}$ |
| 8 | $1.39257 \times 10^{6}$ | $1.39257 \times 10^{6}$ | $-4.13890 \times 10^{-2}$ |
| 9 | $2.57326 \times 10^{6}$ | $2.57378 \times 10^{6}$ | $-5.20943 \times 10^{2}$ |

is ignored; however, it is hard to guarantee that the operation policy is free of problems.

To finish with, we evaluated the independent energy inflow case considering the *fc* corrections with linear (Fig. 13) and quadratic approximations of the EER attributes (Fig. 14). The objective is to show that the *fc* correction is only a problem when the energy inflow is a state variable, i.e., the energy inflow at a particular node is dependent on of its ancestor node.

To sum up, Table 4 presents the worst result in each case, which is the biggest difference between the upper and lower bound in all 10 seeds. It is noticeable that the convergence only occurs in the cases that are linear and every time that we add nonlinearity, either in the EER or PAR model, the convergence cannot be guaranteed.

## 6. Conclusions

In this paper we presented the SMERA model, which has being developed by the authors for solving the LTHS problem. The theoretical references used in SMERA are the same of the NEWAVE. By means of this research project we found some shortcomings caused by nonlinearities introduced in the problem formulation, which may not guarantee that the SDDP algorithm produces an optimal policy. Therefore, we discussed those problems and presented possible solutions that were implemented so far. It is important to point out that even though these issues are part of the LTHS problem, the Brazilian operation seems be fine, since this model is only one part of the scheduling procedure.

In order to guarantee that SMERA was working as expected, we firstly validated it by considering independent Energy Inflows. In the sequence the problem was solved by the SMERA model and by means of a single LP. After confirming that the SMERA was able to produce coherent results, it was shown that the nonlinearities cause problems to the SDDP algorithm, because invalid Benders cuts were added to the model. We evaluated one alternative to deal with the EER nonlinear attributes, which was very simple and effective solution.

Additionally, two approaches were suggested in this paper to substitute the PAR model, the Independent model and the PAR model with $\delta^{MAX}$. These approaches produced good results in terms of the nonlinearities in the LTHS problem; however, the Independent model does not replicate the historical time series and the PAR model with $\delta^{MAX}$ does not allow re-sample, which is important for the SDDP strategy. The re-sampling requires a $\delta^{MAX}$ that would be prohibitively big; otherwise, it could generate negative Energy Inflows. Therefore, the solutions for the PAR model cannot be considered final solutions.

This paper aimed to present the SMERA model to optimization community and show that the nonlinearities introduced in the LTHS problem formulation may produce unsatisfactory results. We presented strategies to deal with some of the problems and we are currently studying other ways to overcome the remaining problems.

## Acknowledgement

Research supported by Conselho Nacional de Desenvolvimento Científico e Tecnológico (CNPq) and Agência Nacional de Energia Elétrica (ANEEL) through projects of Research & Development.

## References

[1] Homem-de-Mello T, de Matos V, Finardi E. Sampling strategies and stopping criteria for stochastic dual dynamic programming: a case study in long-term hydrothermal scheduling. Energy Syst 2011;2:1–31.
[2] de Matos VL, Philpott AB, Finardi EC, Guan Z. Solving long-term hydrothermal scheduling problem. 17th power systems computation conference. Stockholm; 2011.
[3] dos Santos MLL, da Silva EL, Finardi EC, Gonçalves REC. Practical aspects in solving the medium-term operation planning problem of hydrothermal power systems by using the progressive hedging method. Int J Electr Power Energy Syst 2009;31:546–52.
[4] Gonçalves REC, Finardi EC, Silva ELd. Applying different decomposition schemes using the progressive hedging algorithm to the operation planning problem of a hydrothermal system. Electr Power Syst Res 2012;83:19–27.
[5] Gonçalves REC, Finardi EC, Silva ELd, Santos MLLd. Comparing stochastic optimization methods to solve the medium-term operation planning problem. Comput Appl Math 2011;30:289–313.
[6] Finardi EC, da Silva EL. Solving the hydro unit commitment problem via dual decomposition and sequential quadratic programming. IEEE Trans Power Syst 2006;21:835–44.

[7] Saber AY. Economic dispatch using particle swarm optimization with bacterial foraging effect. Int J Electr Power Energy Syst 2012;34:38–46.
[8] Vaisakh K, Praveena P, Rama Mohana Rao S, Meah K. Solving dynamic economic dispatch problem with security constraints using bacterial foraging PSO-DE algorithm. Int J Electr Power Energy Syst 2012;39:56–67.
[9] Lyu JK, Kim MK, Yoon YT, Park JK. A new approach to security-constrained generation scheduling of large-scale power systems with a piecewise linear ramping model. Int J Electr Power Energy Syst 2012;34:121–31.
[10] Mahor A, Rangnekar S. Short term generation scheduling of cascaded hydro electric system using novel self adaptive inertia weight PSO. Int J Electr Power Energy Syst 2012;34:1–9.
[11] Catalão JPS, Pousinho HMI, Mendes VMF. Scheduling of head-dependent cascaded reservoirs considering discharge ramping constraints and start/stop of units. Int J Electr Power Energy Syst 2010;32:904–10.
[12] Wood AJ, Wollenberg BF. Power generation, operation, and control. New York: Wiley; 1984.
[13] Pereira MVF, Pinto LMVG. Multi-stage stochastic optimization applied to energy planning. Math Program 1991;52:359–75.
[14] Maceira MEP, Mercio CMVDB, Gorenstin GB, Cunha SHF, Suanno C, Sacramento MC, et al. Energy evaluation of the North/Northeastern and South/Southeastern interconnection with NEWAVE model. Symposium of Specialists in Electric Operational and Expansion Planning – SEPOPE. Salvador, BA, Brasil; 1998.
[15] Sherkat VR, Campo R, Moslehi K, Lo EO. Stochastic long-term hydrothermal optimization for a multireservoir system. IEEE Trans Power Appar Syst 1985;PAS-104:2040–50.
[16] Kumar ABR, Vemuri S, Ebrahimzadeh P, Farahbakhshian N. Fuel resource scheduling – the long-term problem. IEEE Trans Power Syst 1986;1:145–51.
[17] Archibald TW, Buchanan CS, Thomas LC, McKinnon KIM. Controlling multi-reservoir systems. Eur J Oper Res 2001;129:619–26.
[18] Escudero LF, de la Fuente JL, Garcia C, Prieto FJ. Hydropower generation management under uncertainty via scenario analysis and parallel computation. IEEE Trans Power Syst 1996;11:683–9.
[19] Jacobs J, Freeman G, Grygier J, Morton D, Schultz G, Staschus K, et al. SOCRATES: a system for scheduling hydroelectric generation under uncertainty. Ann Oper Res 1995;59:99–133.
[20] Castro J, González JA. A nonlinear optimization package for long-term hydrothermal coordination. Eur J Oper Res 2004;154:641–58.
[21] Soares S, Carneiro AAFM. Optimal operation of reservoirs for electric generation. Power Delivery, IEEE Transactions on. 1991;6:1101–7.
[22] Pereira MVF, Campodónico N, Kelman R. Application of stochastic dual DP and extensions to hydrothermal scheduling. Rio de Janeiro: PSRI; 1999.
[23] Silva EL, Finardi EC. Planning of hydrothermal systems using a power plant individualistic representation. Power Tech Proceedings, IEEE Porto 2001;3:6.
[24] Silva ELd, Finardi EC. Parallel processing applied to the planning of hydrothermal systems. IEEE Trans Parallel Distrib Syst 2003;14:721–9.
[25] de Matos VL, Finardi EC, Silva ELd. Comparison between the energy equivalent reservoir per subsystem and per cascade in the long-term operation planning in Brazil. EngOpt – international conference on engineering optimization. Rio de Janeiro; 2008.
[26] dos Santos MLL, Silva ELd, Finardi EC. Solving the short term operating planning problem of hydrothermal systems. 16th Power systems computation conference. Glasgow; 2008.
[27] Shapiro A, Philpott AB. A tutorial on stochastic programming; 2009.
[28] Arvanitidits NV, Rosing J. Composite representation of a multireservoir hydroelectric power system. IEEE Trans Power Appar Syst 1970;PAS-89:319–26.
[29] CEPEL. Manual de Referência do Modelo NEWAVE. Rio de Janeiro: CEPEL; 2001.
[30] Noakes DJ, McLeod I, Hipel KW. Forecasting monthly riverflow time series. Int J Forecast 1985;1:179–90.
[31] Hipel KW, McLeod AI. Time series modelling of water resources and environmental systems. Amsterdam; New York: Elsevier; 1994.
[32] Philpott AB, Guan Z. On the convergence of stochastic dual dynamic programming and related methods. Oper Res Lett 2008;36:450–5.
[33] Infanger G, Morton DP. Cut sharing for multistage stochastic linear programs with interstage depency. Math Program 1996;75.
[34] Chiralaksanakul A, Morton DP. Assessing policy quality in multi-stage stochastic programming: Humboldt-Universität zu Berlin, Institut für Mathematik; 2004.
[35] Charbeneau RJ. Comparison of the two- and three-parameter log normal distributions used in streamflow synthesis. Water Resour Res 1978;14.
[36] Benders JF. Partitioning procedure for solving mixed variables programming problems. Numer Math 1962;4:238–52.